



### Science Arts & Métiers (SAM)

is an open access repository that collects the work of Arts et Métiers Institute of Technology researchers and makes it freely available over the web where possible.

This is an author-deposited version published in: <https://sam.ensam.eu>  
Handle ID: [.http://hdl.handle.net/10985/14738](http://hdl.handle.net/10985/14738)

#### To cite this version :

Romain GUIHEUX, Denis BOUSCAUD, Etienne PATOOR, Quentin PUYDT, Pierre OSMOND, Bastien WEBER, Sophie BERVEILLER, Regis KUBLER - Shot Peening Analysis on Trip780 Steel Exhibiting Martensitic Transformation - In: International Conference on Shot Peening, Canada, 2017-09 - ICSP13 - 2017

Any correspondence concerning this service should be sent to the repository

Administrator : [scienceouverte@ensam.eu](mailto:scienceouverte@ensam.eu)





### **Science Arts & Métiers (SAM)**

is an open access repository that collects the work of Arts et Métiers ParisTech researchers and makes it freely available over the web where possible.

This is an author-deposited version published in: <https://sam.ensam.eu>  
Handle ID: <http://hdl.handle.net/null>

#### **To cite this version :**

Romain GUIHEUX, Sophie BERVEILLER, Régis KUBLER, Denis BOUSCAUD, Etienne PATOOR, Quentin PUYDT, Pierre OSMOND, Bastien WEBER - Shot Peening Analysis on Trip780 Steel Exhibiting Martensitic Transformation - In: International Conference on Shot Peening, Canada, 2017-09 - ICSP13 - 2017

Any correspondence concerning this service should be sent to the repository

Administrator : [archiveouverte@ensam.eu](mailto:archiveouverte@ensam.eu)



### Shot peening analysis on trip780 steel exhibiting martensitic transformation

R. Guiheux <sup>a</sup>, S. Berveiller <sup>b</sup>, R. Kubler <sup>c</sup>, D. Bouscaud <sup>b</sup>, E. Patoor <sup>d</sup>, Q. Puydt <sup>a</sup>, P. Osmond <sup>e</sup>, B. Weber <sup>f</sup>

Institut de Recherche Technologique M2P, France, romain.guiheux@irt-m2p.fr, quentin.puydt@irt-m2p.fr

<sup>b</sup> Arts et Métiers ParisTech, LEM3, France, sophie.berveiller@ensam.eu, denis.bouscaud@ensam.eu

<sup>c</sup> Arts et Métiers ParisTech, MSMP, France, <sup>2</sup>regis.kubler@ensam.eu

<sup>d</sup> Georgia Tech Lorraine, France, etienne.patoor@georgiatech-metz.fr

<sup>e</sup> PSA, France, pierre.osmond@mpsa.com

<sup>f</sup> ArcelorMittal Research, France, bastien.weber@arcelormittal.com

**Keywords:** shot peening, residual stresses, TRIP steel, martensitic transformation, finite element simulation.

#### Introduction

In the last years, due to increasing ecology and environmental constraints, a search for lightweight structures has been carried out, leading to the use of more complex geometries and new materials. In that context, TRIP (TRansformation Induced Plasticity) steels are of particular interest as the due to their good mechanical properties to weight ratio [1]. They are often used in the automotive industry for reinforcement parts of the vehicle (bumper, door beam...). To increase life duration, critical parts are shot peened. The specific mechanical behaviour of TRIP steels is due to their microstructure: they contain residual austenite that can transform into martensite when a stress is applied. This mechanism is responsible for hardening of the steels. The beneficial effect of shot peening on metastable austenitic steels was recently established by Fargas et al. [2], resulting in extensive austenite to martensite phase transformation.

Numerous analytical models and numerical approaches based on finite element analysis have been developed to simulate the shot peening process. Reviews of the wide variety of numerical models can be found in Rouhaud et al. [3] and Sherafatnia et al. [4]. Only few experimental studies have been published up to now dealing with the impact of shot peening on metastable austenitic steels [5-7]. The first model taking into account the TRIP effect during peening was proposed very recently by Halilovic et al. [8]; it was developed for an austenitic steel AISI 304 peened steel with a single laser shot using a large strain formulation of transformation plasticity.

#### Objectives

In this study, part of the CONDOR project of IRT M2P, we aimed to study and model the influence of the martensitic transformation occurring during shot peening on the behaviour of a TRIP steel at the phase scale. Shot peening was applied to TRIP 780 steel specimens (2 mm thick, 15% of initial residual austenite) by a Wheelabrator turbine machine for different peening conditions using steel shot media. Residual stresses in each phase and residual austenite fraction was studied after shot peening. A semi-physical numerical model, coupling the mechanical and thermodynamical behaviours, was developed at the scale of the phases following the work of Kubler et al. [9].

The main objective was to understand and predict the effect of shot peening on the mechanical fields in the different phases of TRIP780 steel taking into account plastic hardening and martensitic transformation.

#### Methodology

The studied steel is a cold-rolled commercial TRIP 780 steel provided by ArcelorMittal in the form of a 2 mm thickness sheet. Its chemical composition is provided Table 1; it has a complex microstructure (Figure 1) composed of ferrite, bainite and residual austenite. The volume fraction of austenite is about 15%. The yield strength and ultimate tensile strength are respectively 560 and 780 MPa.

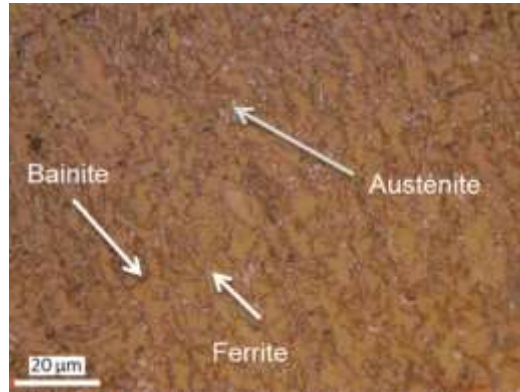


Figure 1: Microstructure of the TRIP 780 steel. Austenite corresponds to white grains.

Table 1: Chemical composition and estimated phase volume fraction [ArcelorMittal data]

Chemical composition (wt%)			Estimated phase volume fraction (%)			
C	Si	Mn	Austenite	Ferrite	Bainite	Martensite
0.209	1.61	1.64	15	70~75	10~15	0

Shot peening (SP) was performed on rectangular samples of 60x60x2 mm<sup>3</sup>, using a Wheelabrator turbine machine. The diameter of the steel shots used was 400 μm, with an exposure time of 16 s. The SP intensity was measured by the arc height of Almen specimens (A type), corresponding to F19A. The coverage rate was 230%. In order to take into account the effect of forming process, SP was performed on two kinds of samples: the as-received one and a pre-strained one obtained by tensile straining at a total strain of 10%.

The retained austenite contents after SP were determined from the X-ray diffraction peak intensities of four hkl planes with Cr-K $\alpha$  radiation: {200} and {220} for the austenite, and {220} and {211} for the BCC phases.

Residual stresses were analysed by X-ray diffraction (XRD), using the classical  $\sin^2\psi$  method (NF EN 15305); residual stress in the austenitic phase was measured using Mn-K $\alpha$  radiation. For the {311} crystallographic planes, the Elastic RadioCrystallographic constants (ERC) values are  $\frac{1}{2} S_2 = 7.18 \times 10^{-6} \text{ MPa}^{-1}$  and  $S_1 = -1.20 \times 10^{-6} \text{ MPa}^{-1}$ . Ferrite, ferrite of the bainite and martensite have quite the same diffraction positions; therefore, it is not possible to separate each contribution. We determine the average residual stress over these phases, named BCC residual stress, using Cr-K $\alpha$  radiation. For the {311} crystallographic planes, the ERC values are  $\frac{1}{2} S_2 = 5.92 \times 10^{-6} \text{ MPa}^{-1}$  and  $S_1 = -1.28 \times 10^{-6} \text{ MPa}^{-1}$ .

In order to get the in-depth profile, material removal was performed by electrolytical polishing in a saline solution. As it may induce a stress relaxation, experimental values of residual stresses were corrected from layer removal using the Sikarskie's correction [10].

## Results and analysis

### Experimental results

Before SP, the retained austenite content was measured at 12% in the as-received steel; residual stresses were homogeneous in both phases and rather weak (lower than 100 MPa). After pre-straining, the austenite content has decreased to 9%. Residual stresses of about 20 MPa were obtained in both phases and in both directions (tensile and transverse ones). The hardness has also increased from 270 HV0.3 to 320 HV0.3.

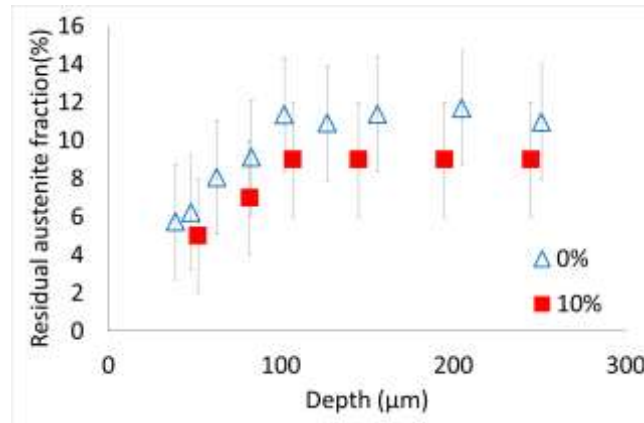


Figure 2: Evolution of residual austenite content as a function of depth for as-received (0%) and pre-strained (10%) samples.

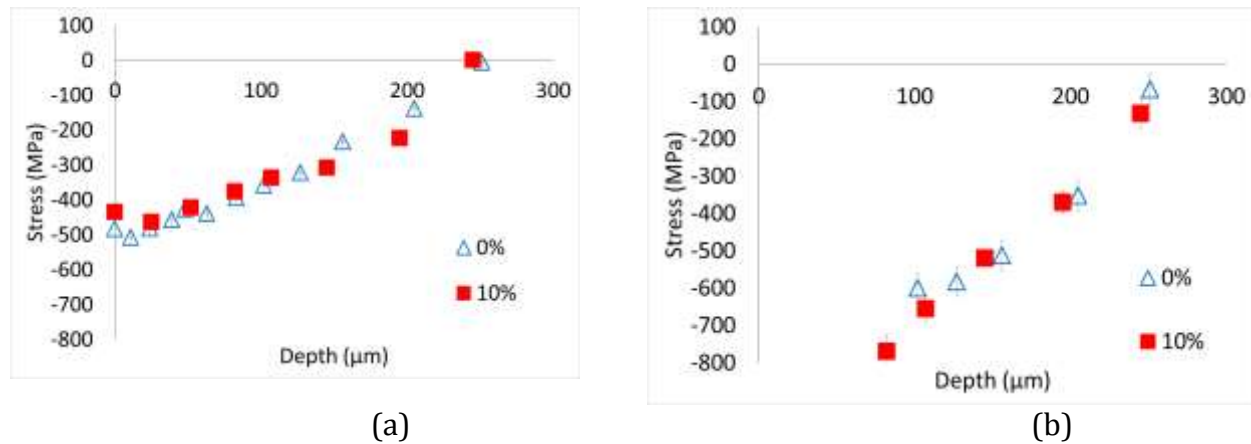


Figure 3: Residual stress profile in the BCC (a) and the FCC (b) phases determined by XRD. In the BCC phases, for the as-received sample, the residual stress state at the surface is in compression (about -490 MPa). It increases to a maximum of -510 MPa at a depth of 15  $\mu\text{m}$ ; then it decreases gradually with increasing depths. It is almost zero at around 250  $\mu\text{m}$ ; tensile values are expected for larger depths. The pre-strained sample shows the same profile. There is only a difference of 50 MPa at the surface. However, considering stress uncertainty, stress values can be assumed the same on both samples, as well as the affected zone depth.

The profile of residual austenite obtained after SP is presented Figure 2 as a function of depth. In the first 40  $\mu\text{m}$  below the surface, the austenite fraction was too low to get an accurate measurement. It is thus estimated less than 3%. The austenite content increases gradually up to the initial value which is reached at a depth of about 120  $\mu\text{m}$ . SP induces the martensitic transformation over one hundred of micrometers. The pre-strain does not influence the affected zone size: the 3% shift observed at large depth corresponds to the austenite transformed into martensite during the previous tensile test. Though the large uncertainties compared to the absolute values, results show that the transformation is maximum at the top surface, within the first 50  $\mu\text{m}$ .

Figure 3 shows the residual stress profile in the BCC (a) and the FCC (b) phases determined by XRD. In the BCC phases, for the as-received sample, the residual stress state at the surface is in compression (about -490 MPa). It increases to a maximum of -510 MPa at a depth of 15  $\mu\text{m}$ ; then it decreases gradually with increasing depths. It is almost zero at around 250  $\mu\text{m}$ ; tensile values are expected for larger depths. The pre-strained sample shows the same profile. There is only a difference of 50 MPa at the surface. However, considering stress uncertainty, stress values can be assumed the same on both samples, as well as the affected zone depth.

Due to the weak intensity of the austenite peaks, no accurate measurements could be obtained in the first 50  $\mu\text{m}$  as for the fraction measurement. As stress correction from material removal

requires the knowledge of the surface stress value, we were not able to perform it. So values are the measured ones, not the corrected ones as for the BCC phases. Austenite exhibits also compression state: at a 100  $\mu\text{m}$  depth, the stress of the as-received sample is -600MPa; this compression value is larger than in the BCC phases (-490MPa at the top surface). The stress decreases gradually with increasing depths and becomes almost zero at 250 $\mu\text{m}$  as for the BCC phases. The stress decrease seems to be faster for depths larger than 120 $\mu\text{m}$ . This inflexion point corresponds to the depth where the austenite content has increased back to its initial value. Therefore, the austenite stress state is rather constant in the zone affected by the martensitic transformation and varies much more when the austenite is stable. However this effect seems to be less pronounced on pre-strained samples; it would be of interest to have more measurements to confirm this issue.

### Numerical simulation

A semi-physical numerical model, coupling the mechanical and thermodynamical behaviours, was developed at the scale of the phases following the work of Kubler et al. [9]. It consists in a thermo-elastoplastic model with phase transformation. A Representative Volume Element (RVE) of a set of four components was selected in order to model the behaviour of the steel: ferrite, bainite, residual austenite and martensite. Complete description of the model can be found in [11]. Thus the mechanical behaviour of each constituent and the martensitic transformation kinetics can be determined.

A finite element simulation of shot peening with consecutive impacts of spherical media has been developed using the specific behaviour law implemented in a VUMAT subroutine in Abaqus Explicit. The dimensions of the simulated sample are large enough to be considered as a semi-infinite medium (Figure 4). Due to symmetry conditions with respect to the (XZ) plane, only one half of the sample was modelled. Four among six lateral faces of the impacted workpiece were constrained in displacement along their normal directions; only the upper impacted surface was set free to deform. The mesh size was chosen to ensure acceptable computational time with regards to a convergence of the residual stress profiles. The mesh is made of hexahedral elements with reduced integration C3D8R in the upper part, and of tetrahedral elements C3D4 in the bottom part.

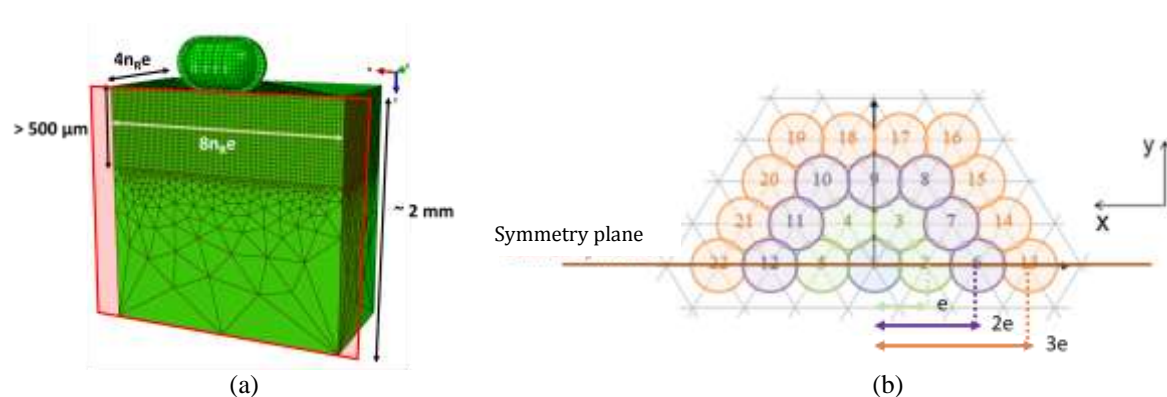


Figure 4: Shot peening simulation. (a): mesh used for calculation. (b): shots distribution at the sample surface. ( $n_R$ : number of shots row impacting the sample)

The shot behaviour is assumed to be elastic. The shots are positioned following a deterministic hexagonal pattern to obtain the experimental coverage rate (230%) according to an analytical law estimating the impact radius. Microstructural and mechanical fields were calculated at a given depth by averaging the corresponding values on all the nodes located at the same depth under the impact zone. The austenite content and residual stresses in each constituent were determined; this allows calculating the macroscopic stress using a mixture law (Figure 5a). In order to compared simulated

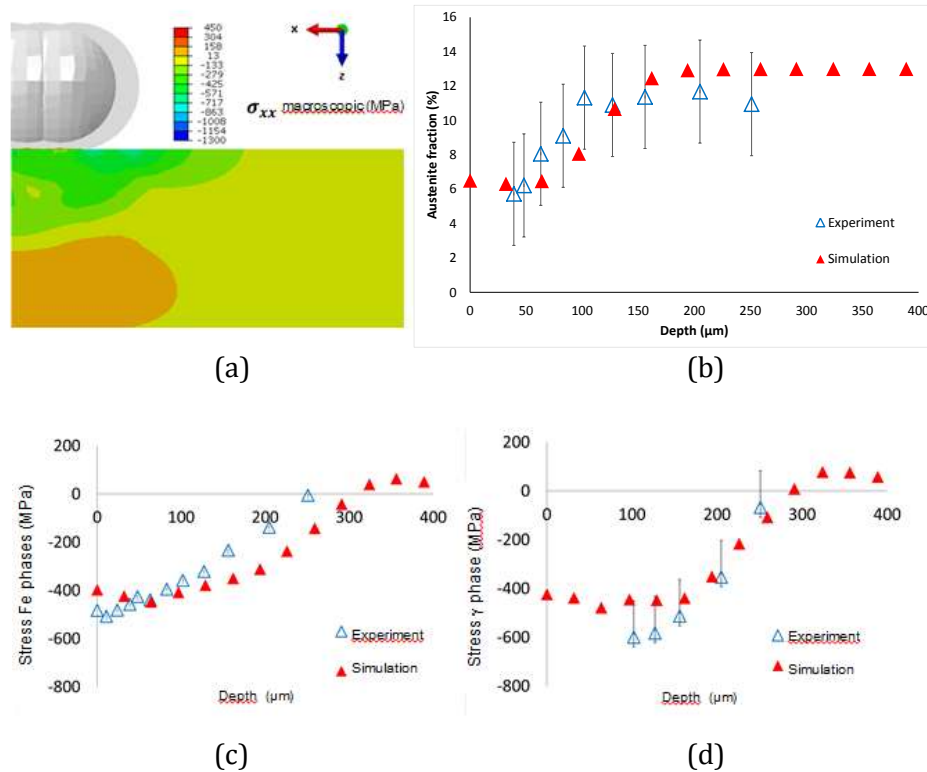


Figure 5: Shot peening of the non-deformed TRIP 780 steel. Simulated macroscopic stress in x direction (a). Experimental vs. simulated austenite volume fraction profile (b), residual stress profiles in the BCC phases (c) and in austenite  $\gamma$  (d).

data with experimental ones in the case of the non-deformed steel, the mean stress over the BCC phases was also calculated (Figure 5c); for austenite, a direct comparison can be made (Figure 5d). Simulated results fit quite well to the experimental austenite fraction; nevertheless a shift of 30  $\mu\text{m}$  is observed: the austenite fraction gets back equal to the initial value at 120  $\mu\text{m}$  (resp. 150  $\mu\text{m}$ ) for experimental (resp. simulated) values. At the top surface, the fraction was too low to be detected by XRD; the model predicts a quite constant value in the first 50  $\mu\text{m}$ , around 5%.

Residual stress profiles are in good agreement with experimental data. The BCC phases stress is decreasing more rapidly when the martensite fraction decreases too. As for the austenite profile, a shift of 30  $\mu\text{m}$  is observed between both profiles. Note that the value at the surface is not well predicted as in many models as it is very sensitive to contact conditions. In the austenite, the difference between experimental and simulated values seems to be higher but one has to keep in mind that experimental values are not corrected from matter removal. If we consider that it should induce an increase of 150 MPa (as in BCC phases), then predicted values are quite good. The advantage of simulation is that it gives access to the entire profile of austenite stress.

### Conclusions

The microstructure and mechanical fields were studied on a cold-rolled TRIP 780 steel after conventional shot peening, and with or without pre-strain; for the first time, results were compared to numerical simulations at the phase scale.

1. The pre-strain does not affect residual stresses in the different phases nor the affected depth but it shifts the austenite fraction value towards lower values.
2. All the constituents were found in compression; the maximum value reached in the austenite was -800 MPa while around -500 MPa in the BCC phases.
3. The stress variations are maximum in the zone affected by the martensitic transformation.

4. A good agreement was obtained with numerical simulation of the martensitic transformation kinetics and residual stresses.

### References

- [1] W.J.Dan, S.H.Li, W.G.Zhang, Z.Q.Lin, *Mater.Des.* 29(3)(2008) 604–612.
- [2] G. Fargas, J. J. Roa, A. Mateo, *Mater. Sci. Eng. A* 641 (2015) 290–296
- [3] E. Rouhaud, D. Deslaef, J. Lu, JL Chaboche. in Jian Lu (Ed.) *Handbook on Residual Stress*, Society of Experimental Mechanics (2005)
- [4] K. Sherafatnia, GH Farrahi, AH Mahmoudi, A. Ghasemi. *Mater. Sci. Eng. A.* 657 (2016) 309-321
- [5] X. Kléber and S. P. Barroso, *Mater. Sci. Eng. A* 527(21-22) (2010) 6046–6052.
- [6] M. Turski, S. Clitheroe, AD Evans, C. Rodopoulos, *Appl. Phys. A* 99 (3) (2010) 549-556.
- [7] P. Fu, K. Zhan, and C. Jiang, *Mater. Des.* 51 (2013) 309–314
- [8] M. Halilovič, S. Issa, M. Wallin, H. Hallberg, and M. Ristinmaa, *Int. J. Mech. Sci.* 111–112 (2016) 24–34.
- [9] RF. Kubler, M. Berveiller, P. Buessler. *Int. J. Plast.* 27 (2011) 299-327
- [10] D. L. Sikarskie, *AIME Met Soc Trans*, 239(4) (1967) 577–580
- [11] R. Guiheux, « Comportement d’aciers à transformation de phase austénite-martensite pour la simulation du grenailage de précontrainte ». Ph.D. Thesis, ENSAM (2016). [www.theses.fr/2016ENAM0055](http://www.theses.fr/2016ENAM0055)